ACADEMIC PRESS

Available online at www.sciencedirect.com
SCIENCE DIRECT®

Journal of Catalysis 214 (2003) 153–164

JOURNAL OF CATALYSIS

www.elsevier.com/locate/jcat

The kinetics of H/D exchange in cyclopentane

M.K. Oudenhuijzen, S. van Dommele, J.A. van Bokhoven, and D.C. Koningsberger *

Department of Inorganic Chemistry and Catalysis, PO Box 80083, 3508 TB Utrecht, The Netherlands

Received 20 June 2002; revised 17 September 2002; accepted 23 September 2002

Abstract

The exchange of hydrogen for deuterium (H/D exchange) in cyclopentane (CP) is a promising test reaction for studying support effects in heterogeneously metal-catalyzed reactions, such as differences in stability and activity in, e.g., benzene or tetralin hydrogenation reactions. In order to employ this test reaction, a full understanding of the H/D exchange mechanism is essential. However, clear insight in the observed kinetics and selectivities is lacking in the literature. In this paper, a kinetic model that adequately describes the observed activity and orders in CP and D_2 is developed. It is shown that the selectivity is determined in a series of reactions after the rate-determining step. To understand the observed selectivities a Monte Carlo model is developed which accurately simulates the observed exchange patterns and reveals the relative contributions of four competitive intermediates. One intermediate (a π-bonded η^2-cyclopentene) can rotate in a nonactivated mechanism via an allylic intermediate. The model reveals the number of rotations each intermediate experiences and can be as high as ~ 20, even if only 5 D atoms are observed in the product. This number of rotations is a better measure of the H/D exchange than the conventional "multiplicity." The H/D exchange of CP together with these insights can now be applied to investigate in detail the influence of the support on the catalytic properties of supported metal particles.

Keywords: Pt catalyst; HD exchange; Pt; Cyclopentane; H_2; Test reaction; Reaction kinetics; Reaction mechanism; Model study

1. Introduction

Numerous reports have been made on the influence of support materials on the activity of supported metal catalysts. For example, activity and selectivity in benzene hydrogenation over zeolite-supported Pt particles largely depend on the support material [1–5]. Another example is the large change in the activity of zeolite-supported Pt catalysts in hydrogenolysis with changing support acidity [6]. If the relation between support material and changes in activity/selectivity is well understood, it offers the prospect of tailor-made catalysts.

A large amount of work has been dedicated to relating changes in catalytic properties to changes in the electronic properties of the Pt particles [5,7–11]. Work by our group has shown that the support results in an electron rearrangement within the metal particle [12]. This rearrangement of electrons consists of a change in the ionization potential of the Pt particles and of a shift in the location of the electrons within the Pt particle.

One of the clearest examples where it is shown that changes in the electronic properties influence the adsorption of reactants on Pt particles is given by the chemisorption of CO followed by infrared spectroscopy. It is observed that CO adsorbs preferentially onto an atop site when the Pt particles are supported by an acidic support, but it adsorbs in the bridged site when basic supports are used [13–17]. In addition, a number of catalytic experiments trying to correlate the changes in electronic properties to the catalytic performance have been published. For example, De Graaf [18] speculated that the kinetics of neopentane hydrogenolysis depends on the degree of dehydrogenation during the adsorption of neopentane on Pt particles. On acidic supports, neopentane adsorbs onto the Pt particle via a single Pt–C bond, and the neopentane loses a single H atom. On basic supports, however, the neopentane adsorbs via double or triple bonds to the Pt clusters, losing an increased number of hydrogen atoms, which could explain the observed variations in the order in H_2 (-1.5 for acidic supports and -2.5 for basic supports). Moreover, the activity of the neopentane conversion shows a compensation effect: an increase

* Corresponding author.
E-mail address: d.c.koningsberger@chem.uu.nl (D.C. Koningsberger).

0021-9517/03/$ – see front matter
doi:10.1016/S0021-9517(02)00077-5

in the activation energy E_{app} (which is observed when the basicity of the support is increased) is compensated for by an increase of the preexponential factor lnA_{app} [19]. Bond et al. indicated that a likely cause of the compensation effect is related to different coverages of the reactants on the Pt surface [19]. This indicates that the adsorption properties of the reactants are influenced by the support acidity [18].

However, there is a lot of discussion on the relations between support material and electronic properties on one hand and the catalytic properties on the other. Thus, the need for a good test reaction is obvious. An important requirement for a proper test reaction is that it should be metal-catalyzed only. Among the possible reactions are the conversion of neopentane [6,18,20,21] and neohexane [22–24] and the isotopic exchange of hydrogen with deuterium in hydrocarbons (H/D exchange) [25–28].

The selectivity of the H/D exchange of cyclopentane (CP) gives direct information about different adsorption modes during the reaction. During the H/D exchange of CP, the hydrogen atoms of cyclopentane are replaced by deuterium atoms. Typically, the H/D exchange of cyclopentane shows several maxima in the product distribution. The products show maxima at 1, 5, or 10 exchanged deuterium atoms (the D1, D5, and D10 products), all resulting from different, competing exchange mechanisms. The resulting product distribution is reported to depend strongly on the support material [29]. Basic supports show high selectivity toward the D10 product [28]. In contrast, neutral supports show mainly the D5 product [30] and acidic supports show a large amount of the D1 product [28]. The dependence of the product distribution on the support is explained by different influences on the different adsorption modes by changes in electronic properties [28]. In order to relate the electronic properties to observed activities and selectivities for different catalysts, it is *crucial* to understand which processes lead to the different products.

The D1 product is produced by the exchange of a single hydrogen atom via a σ-bonded η^1-cyclopentyl (further referred to as σ-η^1; see Fig. 1A). The involved reaction mechanism is proposed to be similar for all D2–D5 products and to proceed via a facile interconversion between the σ-η^1 intermediate and either a double σ-bonded α,β-η^2-cyclopentyl (di-σ-η^2, Fig. 1B) [28,31,32] or a π-bonded η^2-cyclopentene (π-η^2, Fig. 1C) [33]. With the D6–D10 products, the cyclopentane has rolled over from one side of the ring to the other, and also the atoms on the second side of the ring are exchanged. The reaction mechanism for this roll-over is proposed to proceed via a double σ-bonded η^1-cyclopentylidene (di-σ-η^1, Fig. 1D) [34].

In the literature, a clear understanding of the H/D exchange of cyclopentane involving all possible exchange mechanisms, dependencies on D_2 and CP partial pressures, and temperature is missing. There still is debate in the literature regarding the D2–D5 products, which are believed to consist of cyclopentane with deuterium atoms all located on a single side of the ring. H/D exchange of CP results in maxima at D1 and D5. It is important to note that it is therefore impossible that the D5 product is produced via a mechanism which involves the same intermediate that results in the D1 product [35].

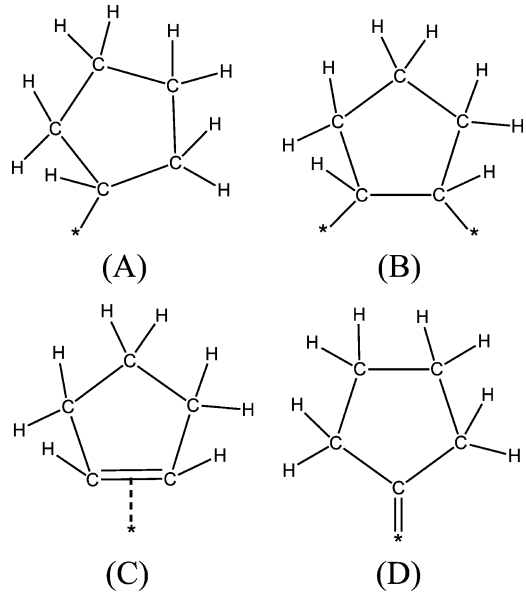

Fig. 1. Different adsorbed intermediates, leading to different products: (A) σ-bonded η^1-cyclopentyl (further referred to as σ-η^1), leading to D1, (B) a double σ-bonded α,β-η^2-cyclopentyl (di-σ-η^2), and (C) π-bonded η^2-cyclopentene (π-η^2) both leading to D2–D5 products, and (D) double σ-bonded η^1-cyclopentylidene (di-σ-η^1), leading to rollover.

This paper will focus on understanding the observed activities and selectivities. A subsequent paper deals with an understanding of support effects on the H/D exchange of CP. As will be shown in this paper, not all exchange mechanisms as proposed in the literature can explain the product distributions as observed for different Pt catalysts. A Monte Carlo-based method that allows for the simulation of exchange patterns has been developed. In addition, a detailed kinetic model, that is able to explain the observed orders and activation energies for the H/D exchange of cyclopentane will be presented.

2. Experimental methods

2.1. Catalyst preparation

A sample of 5 g vacuum-dried SiO_2 (Engelhard, BET surface area 400 m^2/g, pore volume 1.1 ml/g) was impregnated with 5.5 ml of an aqueous solution of $[Pt^{2+}(NH_3)_4](NO_3^-)_2$ (Aldrich, 18.0 mg/ml, resulting in 1 wt% Pt/SiO_2) using the incipient wetness method. The impregnated support was dried in a water-free nitrogen flow for 1 h at room temperature and for 18 h at 80 °C. The resulting catalyst precursor was dried in He for 1 h at 150 °C (ramp 5 °C/min), calcined in 30% O_2/He at 250 °C (ramp 1 °C/min) for 2 h, and reduced at 400 °C for 30 min in H_2 (ramp 1 °C/min) before

the sample was cooled down in He and stored for further use in ambient atmosphere.

The resulting metal particles were analyzed using H_2 chemisorption, high-resolution electron microscopy (HRTEM), and EXAFS. Details are given elsewhere [36,37]. All techniques indicated a similar dispersion. The H_2 chemisorption resulted in $H/Pt_{total} = 0.87$ and $H/Pt_{strong} = 0.43$. HRTEM revealed an upper limit of the metal particle size of 1.7 nm. EXAFS showed a Pt–Pt coordination number (first shell) of 7.8.

2.2. H/D exchange of cyclopentane

A continuous down-flow fixed-bed microreactor (with a diameter of 4 mm) was loaded with 10 mg of the catalyst and diluted with 60 mg of SiO_2, both with a sieve fraction of $90 < d_p < 150$ μm. The catalyst that was previously reduced and stored in ambient atmosphere was again dried at 150 °C in Ar for 1 h and prereduced for 1 h at 400 °C (ramp 5 °C/min) in pure hydrogen. All flows were 30 ml/min, resulting in a gas hourly space velocity of GHSV = 7200 s^{-1} and a contact time of $\tau = 0.5$ s. After the reduction at 400 °C, the H_2 was switched to D_2 and the catalyst was cooled down in 50% D_2 in Ar to 75 °C. Typical H/D experiments were performed at 75 °C at atmospheric pressure, with $P_{D_2} = 0.45$ bar, $P_{CP} = 0.025$ bar (resulting in an atomic ratio of D/H = 20) and $P_{Ar} = 0.475$ bar. The cyclopentane was brought into the feed by flowing part of the Ar through a saturator filled with cyclopentane. Conversions were kept below 10%. No side reactions were observed.

The products were analyzed online by a quadrupole mass spectrometer (Balzers QMS 420) that was connected via a capillary to the outlet of the reactor. The monitored intensities of CP were corrected for the natural abundance of ^{13}C.

Reaction orders in CP and D_2 were determined by varying the pressures ($0.022 < P_{CP} < 0.036$ and $0.33 < P_{D_2} < 0.63$), while the total flow was kept constant. Activation energies were determined by heating the catalyst over a range of 15 °C with a ramp of 1 °C/h, followed by cooling down over (part of) the same temperature range.

The conversion is defined as the total amount of exchanged cyclopentane divided by the total amount of cyclopentane. Selectivity is defined as the amount of a specific product divided by all products,

$$C = 100 * \frac{\sum_{i=1}^{i=10} I_{Di}}{\sum_{i=0}^{i=10} I_{Di}}, \quad (1)$$

$$S_{Di} = 100 * \frac{I_{Di}}{\sum_{i=1}^{10} I_{Di}}, \quad (2)$$

with i—the amount of deuterium atoms in the product and $i = 0$ the unreacted product. C—the conversion (in %). I_{Di}—the amount of product Di (e.g., D3, CP containing three deuterium atoms) detected, after correction for the natural abundance of ^{13}C, and S_{Di}—the selectivity (in %) toward product Di.

In literature, also the "multiplicity" is commonly used to describe the product distribution. This multiplicity M is defined as the average deuterium content in the reacted cyclopentane species according to [35]

$$M = 0.01 * \sum_{i=1}^{i=10} i * S_{Di}, \quad (3)$$

with M—multiplicity, i—number of exchanged deuterium atoms, and S_{Di}—selectivity (%) towards product Di.

3. Results

3.1. Experiments

3.1.1. Influence of D_2 and CP partial pressures

A typical product distribution for the H/D exchange in cyclopentane over a Pt/SiO_2 catalyst, recorded at 73 °C with 10.4% conversion, is shown in Fig. 2. Clearly, three distinct maxima are visible in the selectivity towards the D1, D5, and D10 products.

Fig. 3 shows the influence of the D_2 partial pressure on activity and selectivity. The activity decreases when P_{D_2} is increased (Fig. 3A). Using the power rate law, $r = k P_{CP}^{\alpha} P_{D_2}^{\beta}$, and keeping $k P_{CP}^{\alpha}$ constant, the order of the activity in D_2 was determined at $\beta = -0.85$.

In addition to the activity, also the selectivity depends on P_{D_2} (Fig. 3B). When P_{D_2} was increased, the selectivity toward D1 and D5 increased. D2 was unaffected, and the selectivity towards D3–D4 decreased. The changes in selectivity are also reflected in the multiplicity. It decreases from $M = 4.1$ at low D_2 pressure to $M = 3.7$ at high D_2 pressure.

Fig. 4 shows the influence of the CP partial pressure on the activity and product distribution. The reaction rate is increased by increasing P_{CP}, whereas the selectivity is almost unaffected. Keeping $P_{D_2}^{\beta}$ constant, and using the power rate law, the order of the activity in P_{CP} was determined to be $\alpha = +0.87$.

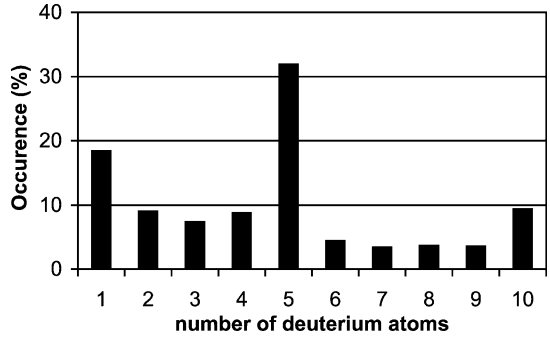

Fig. 2. Typical exchange pattern for Pt/SiO_2 recorded at 73 °C, with 10.4% conversion.

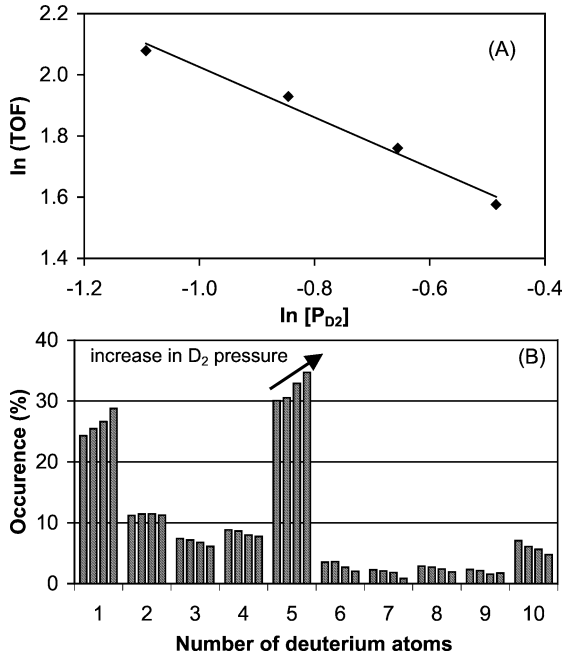

Fig. 3. Influence of the D_2 partial pressure on (A) activity and (B) selectivity.

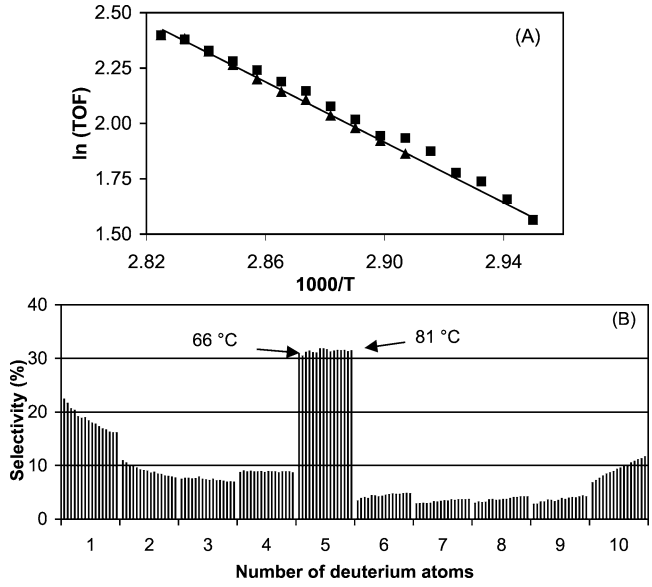

Fig. 5. The influence of temperature on (A) activity and(B) selectivity. (A) Blocks: activity measured during heating from 66 up to 81 °C; triangles: activity during cooling down from 81 down to 71 °C. (B) Distribution normalized for each T at 100%. Left bars: 66 °C; each consecutive bar: +1 °C up to 81 °C.

3.1.2. Effect of temperature

The activity is strongly influenced by the temperature. An Arrhenius plot of the activity as a function of temperature is given in Fig. 5A. Using the Arrhenius law [38], the (apparent) activation energy was determined to be $E_{app} = 55$ kJ/mol.

Fig. 5B shows the influence of the temperature on the selectivity. Increasing the temperature in steps of 1 °C from 66 to 81 °C results in a decrease of the D1, D2, and D3 products and an increase for D6–D10. The selectivity toward D6–D10 increases from 19.1% at 66 °C to 28.8% at 81 °C. D4 and D5 are unaffected. In line with these observations, also the multiplicity increases from $M = 4.4$ at 66 °C to $M = 4.9$ at 81 °C.

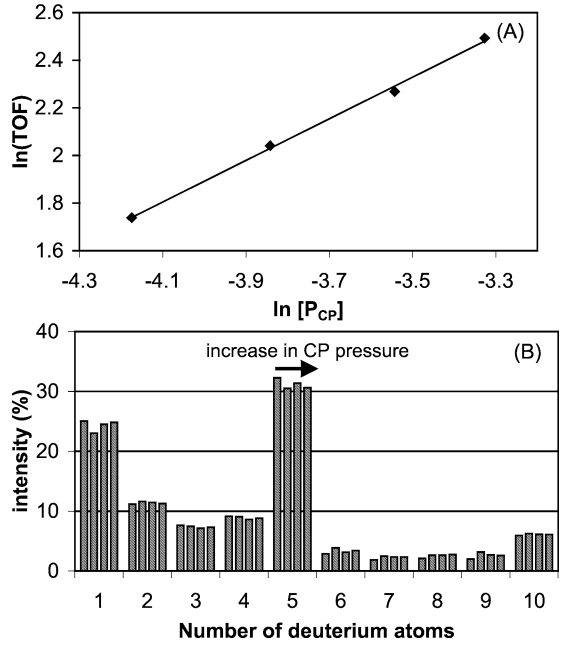

Fig. 4. Influence of the CP partial pressure on (A) activity and (B) selectivity.

3.2. The development of a Monte Carlo model: understanding H/D exchange patterns

As described in literature, a typical exchange pattern (as in Fig. 2, with maxima for D1, D5, and D10) is the result of several competing mechanisms, each resulting in different products.

The mechanisms, as proposed in the literature, proceed via [28,31,34,39,40]:

(1) A single σ-bonded η^1-cyclopentyl intermediate (σ-η^1, Fig. 1A), leading to the D1 product,
(2) A double σ-bonded α,β-η^2-cyclopentyl intermediate (di-σ-η^2, Fig. 1B), leading to D2,
(3) A π-bonded η^2-cyclopentene intermediate (π-η^2, Fig. 1C), responsible for a rotation mechanism and leading to D2–D10, and
(4) A double σ-bonded η^1-cyclopentylidene intermediate (di-σ-η^1, Fig. 1D), responsible for rollover and leading to D6–D10.

3.2.1. The mechanism leading to D1

In the D1 product only one hydrogen atom is exchanged for a deuterium atom. Thus, only one C–H bond is dissociated during adsorption of CP on the Pt. After dissociation,

Pt–C and Pt–H bonds are formed. The most likely form of this Pt–C species is the σ-η^1 intermediate (Fig. 1A) [34,39]. In a competing mechanism, D_2 will be dissociatively chemisorbed on the Pt. This reaction is known to be an easy and fast reaction, with no activation energy [41–44]. Hence, the chemisorbed H-atom on the Pt surface, originating from the cyclopentane, will quickly recombine on the Pt surface with a chemisorbed D-atom to form HD(g). The σ-η^1 intermediate can then recombine with chemisorbed D on the Pt surface, and $C_5H_9D_1$ is formed. This is detected as the D1 product.

3.2.2. The mechanism leading to D2–D5

3.2.2.1. Literature The D2 product itself can easily be formed via the di-σ-η^2 intermediate (Fig. 1B). In addition, it is generally assumed that the D2–D5 products are formed by a stepwise exchange of the D-atoms. Therefore, any mechanism leading to these products must include an adsorption, followed by dissociation and a rotation mechanism, during which the probability of desorption is small compared to the probability of rotating to an adjacent C–C bond.

The mechanism for the rotation reaction has been proposed in literature to involve an alternation between the σ-η^1 intermediate (Fig. 1A) and either a di-σ-η^1 (Fig. 1D) [31,40] or a π-η^2 intermediate (Fig. 1C). However, also D1 is believed to be formed via the σ-η^1 intermediate (Fig. 1A), and thus the amount of D1 observed indicates the desorption probability of the σ-η^1 intermediate. Since generally a (local) maximum for D1 is observed, this desorption probability is relatively high. Therefore, a rotation mechanism involving this σ-η^1 intermediate should show intensities in the order D1 > D2 > D3 > D4 > D5. Since this is not the case, the rotation mechanism cannot include a σ-η^1 intermediate. In addition, since the selectivity towards D5 is much higher than the selectivity to D4, the rotation mechanism must have a low activation energy.

Therefore, another process must be involved in the rotation mechanism which fits the requirements described above. We propose an allylic-like rotation mechanism of a π-bonded species (Fig. 6). This would meet these requirements and is proposed as the mechanism for rotation. In this mechanism, the π-η^2 intermediate is the intermediate molecule which can rotate. The rotations proceed via the formation of an allylic intermediate, and this allylic intermediate breaks

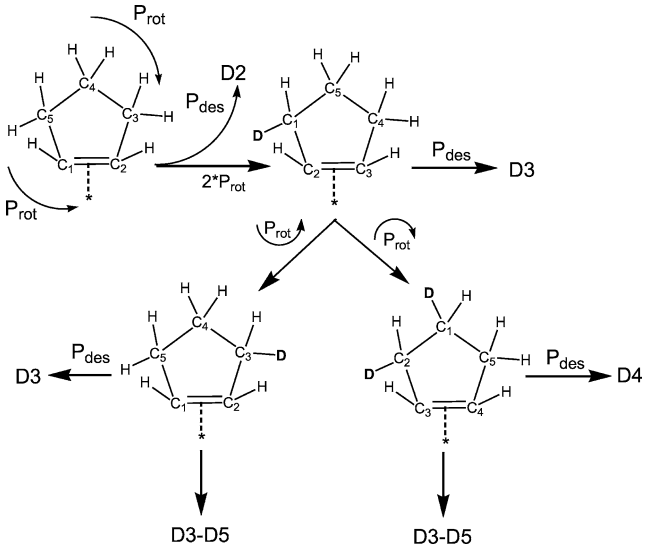

Fig. 7. Schematic representation of the rotation mechanism leading to D3–D5. P_{rot}: probability of rotating either clockwise or counterclockwise, and P_{des}: probability of desorbing. After the first rotation, desorption would yield the D3 product. After the second rotation, desorption can yield both the D3 and D4 products.

a C–H bond and forms a C–D bond on the other side of the allylic bond.

3.2.2.2. Statistics of the rotation mechanism During the initial formation of this rotating intermediate, with a surface coverage θ, two C–H bonds are broken (Fig. 7). This molecule can either recombine with an adsorbed D atom and desorb, or rotate to an adjacent C–C bond. If the molecule would desorb, it would be detected as a D2 product. The desorption probability is given by P_{des}. Now the amount of D2 formed via this π-η^2 intermediate is given by $I_{D2} = \theta P_{des}$. If the molecule rotates, a D atom is attached to one of the C atoms (carbon atom #1 in Fig. 7) and another C atom loses a H atom (C atom #3). Again, the molecule can either desorb or rotate to an adjacent C–C bond. If the molecule desorbs, atoms C_1, C_2, and C_3 have a D atom attached to them and, hence, the molecule would be detected as the D3 product. The adsorbed molecule can also rotate, to either the next C–C bond (the bond between atoms C_3 and C_4 in Fig. 7) or the previous C–C bond (C_1–C_2). The rotation probability in each direction is given by $P_{rot} = \frac{1}{2}(1 - P_{des})$.

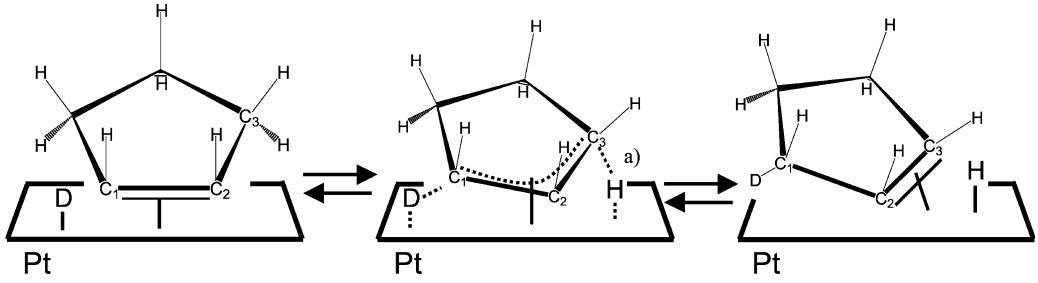

Fig. 6. The rotation mechanism occurs via an allylic intermediate. (a) The hydrogen attached to C3 can either bond to a surface Pt atom or recombine with a chemisorbed D atom to form gaseous HD.

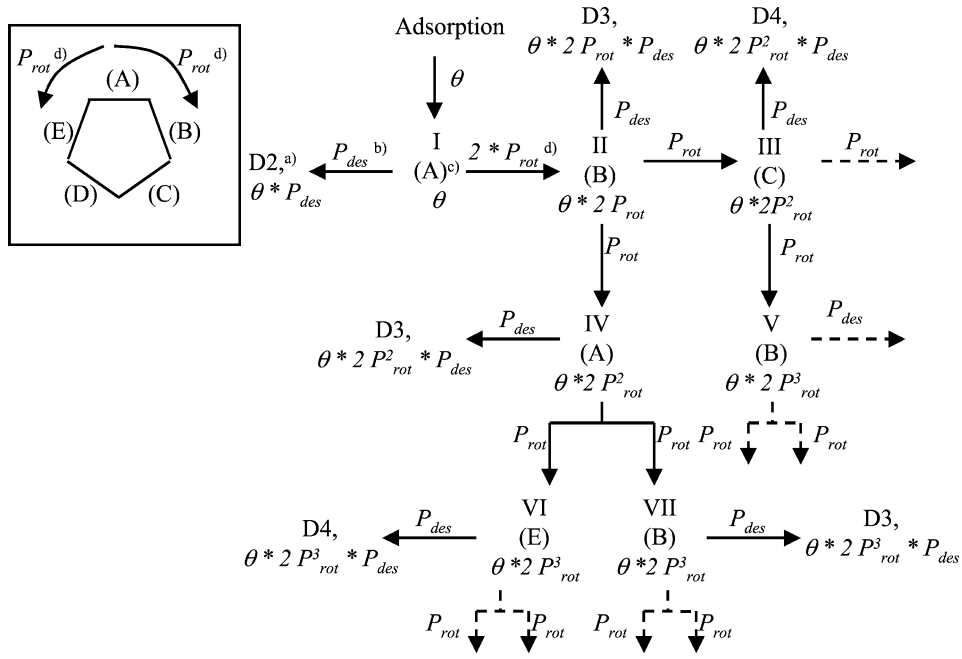

Scheme 1. Statistical approach to the formation of D2–D5 product. (a) The product D2 is formed in a concentration $I_{\mathrm{D2}} = \theta * P_{\mathrm{rot}}$ with θ = surface concentration (in %) of the rotating species and (b): P_{des} = fractional probability on desorption. (c): Species I is bonded at the C–C bond (A). (d): Adsorbed species has a fractional probability P_{rot} of rotating right and an equal probability P_{rot} of rotating left; $P_{\mathrm{rot}} = (1 - P_{\mathrm{des}})/2$. After the first rotation, the species rotated to the left and right are equal. Species VI has been through the following route: adsorption on bond A → B → A → E and desorption would result in the D4 product. The route for species VII has been: A → B → A → B.

In the first case (adsorbed on the C_3–C_4 bond), desorption would lead to a CP molecule with D atoms attached to carbon atoms 1, 2, 3, and 4 and it would be detected as a D4 product. In the latter case (adsorption on the C_1–C_2 bond), however, the C_1–D bond is broken and a C_3–D bond is formed. Desorption then leads to the D3 product with D atoms bonded to C_1, C_2, and C_3. In this D3 molecule four times a C–H or C–D bond has been broken and formed: twice the C_1–H(D) and once the C_2–H and C_3–H bond. This example illustrates that the number of D atoms in the product (three) does not represent the number of times a C–H bond is broken and reconstructed (four times), as is normally assumed in the literature.

A schematic representation of these concepts is shown in Scheme 1. First, a CP molecule is adsorbed as a π-η^2 intermediate, containing 8 H atoms (species I in Scheme 1, adsorbed onto the C–C bond [A]) with a surface concentration θ. This species can either desorb (giving the D2 product) or rotate to an adjacent C–C bond (bond [B] or [E] in Scheme 1). It is important to realize that after the first rotation, desorption of the adsorbed species would yield the D3 product regardless of the direction of rotation. This means that both adsorbed species are indistinguishable: adsorption via C–C bond [B] is indistinguishable from adsorption via C–C bond [E] and, therefore, after one rotation the surface concentration of this species II (Scheme 1) is $2 * \theta * P_{\mathrm{rot}}$.

After the first rotation, the adsorbed molecule goes through a similar mechanism with again the probability P_{des} of desorption (giving an intensity of $I_{\mathrm{D3}} = 2\theta P_{\mathrm{rot}} P_{\mathrm{des}}$) and the probability P_{rot} of rotating to the next C–C bond (bond [C], giving species III in Scheme 1) or the previous C–C (bond [A], species IV) bond. If the molecule would rotate to the previous bond in its second rotation, this molecule would exchange a D-atom for another D-atom, and therefore still be detected as a D3 product, although it would have undergone four exchange steps. This species is depicted in Scheme 1 as species IV, which has undergone adsorption on C–C bond $A \rightarrow B \rightarrow A$. Species IV in Scheme 1 is comparable to the bottom left CP molecule in Fig. 7. When this statistical analysis is followed through (part of which is shown in Scheme 1), it becomes clear that the intensities resulting from the rotation mechanism for the D2 and D3 products are described by

$$I_{\mathrm{D2}} = \theta * P_{\mathrm{des}}, \tag{4}$$

$$I_{\mathrm{D3}} = 2\theta P_{\mathrm{des}} \sum_{n=1}^{\infty} P_{\mathrm{rot}}^{n} = 2\theta P_{\mathrm{des}} \sum_{n=1}^{\infty} \left(\frac{1 - P_{\mathrm{des}}}{2} \right)^{n}, \tag{5}$$

with I_{Di}—the intensity of *Di*, θ—surface coverage (in %) of the rotating species, P_{des}—fractional desorption probability, $P_{\mathrm{rot}} = \frac{1}{2} * (1 - P_{\mathrm{des}})$—probability of rotation, either counterclockwise or clockwise, and n—number of rotations.

3.2.2.3. The development of the Monte Carlo model Such formulas for the D4 and D5 products are very complicated to derive. Therefore, another approach is chosen: the use of Monte Carlo techniques. Since the contribution of a molecule that has undergone a large number (e.g., 20) of rotations to the formation of the D3 product is negligible,

$\theta * P_{\mathrm{des}}$ can be determined from a known intensity of D3 via formula (5). With the known value of $\theta * P_{\mathrm{des}}$, both θ and P_{des} can be estimated separately. The estimation can be checked with the use of a computer code: in this code a CP molecule is virtually adsorbed and rotated randomly until it is desorbed again. With the use of this random generator, the molecule is rotated a number of times and the average number of rotations depends on the estimated value of P_{des}. When the adsorption of a high amount of molecules ($>10^6$) is simulated, a complete exchange pattern can be simulated. In an iterative process toward best agreement between theory and experiment the best values of θ and P_{des} are determined. In Table 1, a comparison between experiment and theory is given. As becomes clear, even though a molecule might be detected as D5, the average number of rotations this molecule has experienced in this particular example is as high as 18.3. Since the adsorbed, unrotated π-η^2 intermediate already yields the D2 product, the average number of exchange steps (one exchange step is defined as a subsequent cleavage and formation of a C–H or C–D bond) is as high as $18.3 + 2 = 20.3$. This gives a good measure for the exchange activity via rotation.

The high amount of D5 product that is (generally) found shows that rotating is easier than desorption. Therefore, P_{des} must be much smaller than P_{rot} ($P_{\mathrm{des}} \ll P_{\mathrm{rot}}$). From formulas (4) and (5) it follows that in this case the contribution of this rotation-mechanism to the D2 product must be smaller than the total amount of the D3 product formed. Since it is generally found that D2 > D3 (Fig. 2), a second mechanism must contribute to the formation of D2. Such a mechanism must include the exchange of two hydrogen atoms and must exclude the possibility of a easy rotation. The di-σ-η^2 intermediate (Fig. 1B) is such a species, and it is proposed that the second mechanism leading to the D2 product proceeds via this di-σ-η^2 intermediate.

In summary, the assumptions made in the development of the Monte Carlo model are:

- The probabilities of rotating clockwise or counterclockwise are always equal. Due to the kinetic isotope effect, these probabilities are in reality not entirely equal when a C–D bond has to be broken in one direction, and a C–H bond has to be broken in the other direction, which is the case only in the initial steps of the exchange reaction. The respective bond strengths differ by only a few percent, and the majority of the exchange steps involve a fully exchanged side of the CP ring where only C–D bonds are present. Therefore the kinetic isotope effect can be safely ignored.
- Already after the initial formation of the rotating species, two D-atoms are exchanged.
- The desorption probability is not influenced by the number of D-atoms in the product.

Table 1
Comparison between theory and the results of the statistical simulation

	D1	D2, di-σ-η^2 [a]	D2, π-η^2 [b]	D2 total	D3	D4	D5	> D5
Experiment	18.4[c]			9.0	7.4	8.8	31.9	24.4
Theory	18.6	2.3	4.6	6.9	7.6	8.9	33.6	24.4
(Number of rotations)[d]					(3.9)	(6.6)	(18.3)	

[a] The amount of D2 produced via the double σ-bonded α,β-cyclopentyl (Fig. 1B).
[b] The amount of D2 produced via the π-bonded cyclopentenyl (Fig. 1C).
[c] Selectivity in %.
[d] The average number of rotations the molecule has experienced.

3.2.3. The mechanism leading to D6–D10

The products D6–D10 have exchanged deuterium atoms on both sides of the cyclopentane ring. These products must have undergone a rollover mechanism which exposes both sides of the ring. The relative intensities D7–D10 and D3–D5 show a similar pattern. This suggests that the formation of the D6–D10 species involves the same intermediate that is responsible for the rotation: the π-η^2 intermediate. Thus, it is the π-η^2 intermediate that can rollover. Therefore, the total amount of the mechanism that proceeds via the π-η^2 intermediate is given by the sum of all products D3–D10 and that part of the D2 product which is formed via the π-η^2 intermediate (Fig. 1B) as calculated with the Monte Carlo model. The activity R_{rollover} for this rollover mechanism is then given by:

$$R_{\mathrm{rollover}} = \frac{\sum \mathrm{D6\text{-}D10}}{\mathrm{D2}_{\pi\text{-species}} + \sum \mathrm{D3\text{–}D10}}. \tag{6}$$

The observation that D6 is more abundant than D7 gives important information on the rollover mechanism [31]. When the intermediate adsorbed species is formed during the rollover, the cyclopentane can either roll back to the same side of the ring or roll forward to the next side of the ring. The relatively high abundance of D6 suggests that the formation of the intermediate involves the cleavage of one C–H bond on the unexchanged side of the ring: if it would roll back, than only one atom would be present on the second side of the ring. This indicates that the dominant mechanism for the rollover is via a di-σ-η^1 intermediate (Fig. 1D) [31]. The D7–D10 product distribution is similar to the D2–D5 distribution, which indicates that for the formation of the D6–D10 products the rollover occurs starting from the π-η^2 (Fig. 1C), via the di-σ-η^1 intermediate (Fig. 1D) toward again the π-η^2 intermediate. Via this mechanism a large number of H atoms can be exchanged for D atoms, leading to the D6–D10 products.

3.2.4. Implications for interpretation of the selectivity

In the literature, the multiplicity has been used to reflect the average number of exchange steps leading to a particular exchanged product. However, the multiplicity does not reflect the full magnitude of changes in the selectivity. It is an overall parameter which is most sensitive for the rollover

Table 2
The influence of the D_2 partial pressure on the selectivity and on the average number of rotations, as calculated with the Monte Carlo method

P_{D_2}[a]	Contribution (in %)[b]				Average number of rotations[c]	M[d]
	σ-η^1 (D1)	di-σ-η^2 (D2)	π-η^2 (D2–D10)	di-σ-η^1 (D6–D10)		
0.34	24.3	3.4	72.3	18.1	12.5	4.1
0.43	25.5	3.7	70.9	16.7	12.9	4.0
0.52	26.7	3.7	69.7	14.2	14.2	3.9
0.62	28.7	3.8	67.5	11.4	15.9	3.7

[a] Partial pressure of D_2.
[b] For a description of the intermediate species, see Fig. 1.
[c] The average number of rotations each π-η^2 intermediate experiences.
[d] Multiplicity.

mechanism leading to D10 and, for example, it only reflects the *observed* number of exchange steps, not the *true* number of exchange steps leading to D5.

It is very likely that the different adsorption modes shown in Fig. 1 are influenced differently by changes in temperature and partial pressure of reactants. The same holds for the influence of support-induced changes in the electronic properties of the metal on the adsorption of the various intermediates. Instead of using the multiplicity, one should carefully analyze the observed selectivities and extract the contribution of the different adsorption modes in the exchange reaction. D1 represents the contribution of the σ-η^1 intermediate. By using the developed Monte Carlo model, the contribution to the formation of D2 of the di-σ-η^2 intermediate can be calculated, as well as the total amount of the π-η^2 intermediate formed and the average number of rotations that each π-η^2 intermediate experiences. The contribution of the rollover mechanism, with the di-σ-η^1 intermediate, follows from Eq. (6).

In order to further illustrate this very important point, the data presented in Table 2 are considered. By increasing the D_2 partial pressure, the multiplicity was decreased by 10%, from 4.1 to 3.7. This is mainly caused by a strong decrease in the rollover activity, from 18.1 to 11.4%. However, the average number of rotations each adsorbed π-η^2 intermediate undergoes is increased by 25%, from 12.5 to 15.9.

4. Discussion

4.1. Orders in D_2 and cyclopentane

By varying the partial pressure of CP while keeping P_{D_2} constant, and assuming the power rate law $r = kP_{CP}^{\alpha}P_{D_2}^{\beta}$, our results show that the order in CP is $\alpha = 0.87$. Remarkably, the selectivity to a particular product is—within accuracy limits—hardly affected by P_{CP}. The observation that all D1–D10 products are unaffected by P_{CP} suggests that all reaction mechanisms leading to the different products have similar rate-determining steps and that the selectivity to the D1–D10 products is only determined *after* the rate-determining steps. This argument and the consideration that a molecule of CP can only be deuterated and observed after a dissociation step of a C–H bond in the CP molecule suggest that the rate-determining step is a dissociation. The first step in a catalytic reaction is always an adsorption of the reactant onto the catalytically active surface. This adsorption step might even precede the rate-determining step. For the adsorption of a hydrocarbon adsorption such as CP onto a Pt surface, the first step adsorption can be either dissociative or molecular adsorption.

Dissociative adsorption can proceed in different ways. Dissociative adsorption during which both CP and a H atom are adsorbed onto the catalytically active surface,

$$C_5H_{10}(g) + 2^* \Leftrightarrow C_5H_9(^*) + H(^*),$$

and a dissociative adsorption onto a site which is filled with a deuterium atom, during which immediately the gaseous HD is formed

$$C_5H_{10}(g) + D(^*) \Leftrightarrow C_5H_9(^*) + HD(g).$$

During this dissociative adsorption atomically adsorbed D is also involved. If this reaction took place, the presence of D_2 would be expected to be beneficial to the reaction rate. However, the order in D_2 for conversion of cyclopentane to any product was determined at $\beta = -0.85$ (see Fig. 3A): the H/D exchange is inhibited by D_2. This is in agreement with reported literature values [45]. Because the order in D_2 is negative, a dissociative adsorption on a site containing $D(*)$ can be excluded.

Also a molecular adsorption in the first step can take place

$$C_5H_{10}(g) + {}^* \Leftrightarrow C_5H_{10}(^*).$$

This is in agreement with a study reported by Campbell and Campbell [46], who showed that, initially, cyclopentane is molecularly adsorbed before it dissociates. The negative order for the activity in D_2 also indicates that both cyclopentane and deuterium adsorb onto the same adsorption sites.

Based on the molecular adsorption in the first step, a series of reactions can be postulated that can explain the observed kinetics:

$$C_5H_{10}(g) + {}^* \overset{K_1}{\longleftrightarrow} C_5H_{10}(^*), \quad \text{(I)}$$

$$D_2(g) + 2^* \overset{K_2}{\longleftrightarrow} 2D(^*), \quad \text{(II)}$$

$$C_5H_{10}(^*) + {}^* \overset{k_{+3}}{\longrightarrow} C_5H_9(^*) + H(^*), \quad \text{(IIIA)}$$

$$C_5H_nD_{9-n}(^*) + D(^*) \overset{k_{-3}}{\longrightarrow} C_5H_nD_{10-n}(^*). \quad \text{(IIIB)}$$

As argued above, all exchange mechanisms, leading to D1–D10, are assumed to originate from the same, dissociatively adsorbed molecule via a series of exchange mechanisms. This is depicted in an energy scheme which is shown in Fig. 8. The highest activation energy is in the rate-determining step, the dissociation of CP. From this dissociated molecule the CP can further react to, for example,

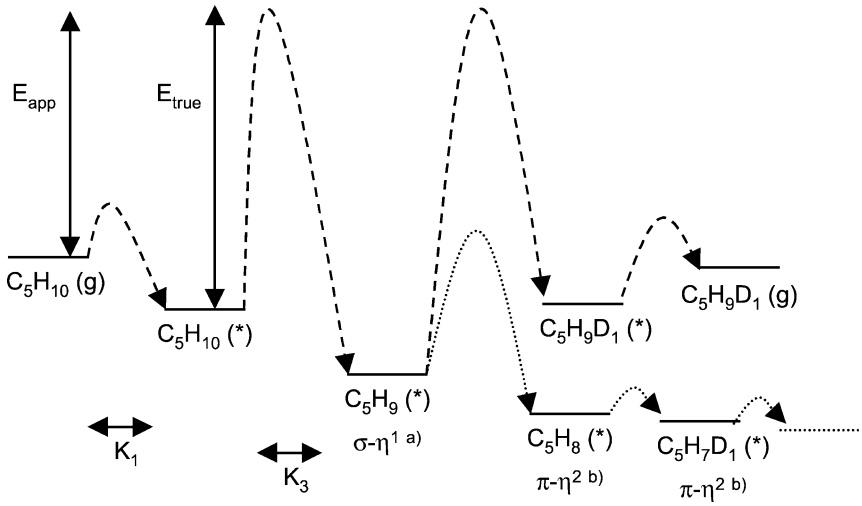

Fig. 8. A schematic energy scheme for the HD exchange of CP. The rate-determining step is K_3, the dissociation of molecularly adsorbed CP to $C_5H_9(^*)$, the (a) σ-bonded η^1-cyclopentyl intermediate. From this dissociated CP the other intermediates are formed, for example (b) π-bonded η^2-cyclopentene. This intermediate can easily rotate with a low activation energy. E_{app} is the apparent (or observed) activation energy, E_{true} the true activation energy.

π-η^2 with a relatively low activation energy. The π-η^2 intermediate can then easily rotate with an even lower activation energy.

As shown in Appendix A, reactions (I)–(III) lead to a reaction rate given by

$$R = \frac{k_{-3}K_1K_3P_{CP}}{\left(1 + K_1P_{CP} + \frac{K_1K_3P_{CP}}{\sqrt{K_2P_{D_2}}} + \sqrt{K_2P_{D_2}}\right)^2}. \quad (7)$$

Reaction (II) involves the dissociation of deuterium on Pt. Since this reaction is known to be fast and nonactivated [41], it is very likely that the equilibrium in this reaction is far to the right side. Moreover, since this reaction is fast, any adsorbed H(*) formed from the dissociation of CP immediately recombines with D(*) to form HD(g). Also, H(*) and D(*) are chemically equal and thus H(*) in reaction (IIIA) can be replaced by D(*), and similarly $C_5H_nD_{9-n}(^*)$ can be replaced by $C_5H_9(^*)$. As a consequence, reactions (IIIA) and (IIIB) are in equilibrium and in a steady state $r_{+3} = r_{-3}$.

Reaction (I) only involves nondissociative adsorption. Therefore, it is expected that $K_2 \gg K_1$ and the denominator in Eq. (7) is dominated by the term $K_2P_{D_2}$. In that case, the observed order in deuterium will be near -1 and the order in CP will be close to $+1$. This is indeed observed in the experiment, with an order of -0.82 in D_2 and $+0.87$ in CP.

In addition to the activity, the selectivity is also influenced by P_{D_2} (Fig. 3B). The selectivities to D1 and D5 increased, D2 was unaffected, and D3, D4, and D6–D10 decreased in intensity with increasing P_{D_2}. These selectivities were analyzed with the Monte Carlo model, and the results are given in Table 2. The contribution of the σ-η^1 intermediate (Fig. 1A) increased, whereas the contribution of the π-η^2 intermediate (Fig. 1C) decreased. In contrast, the average number of rotations which the π-η^2 intermediate experiences increases from 12.5 at low D_2 pressure to 15.9 at higher D_2 pressures. This increase in the average number of rotations suggests that the rotation mechanism is facilitated by an adsorbed D-atom. This is in agreement with the proposed allylic mechanism (Fig. 6): in order to rotate via the resonant mechanism, a deuterium atom must be adsorbed onto an adjacent adsorption site. With higher P_{D_2} the coverage with deuterium is expected to be higher and, hence, the rotation is more facile.

The contribution of the di-σ-η^1 intermediate decreases from 18.1 to 11.3% with increasing D_2 pressure. This means that the rollover, which results in D6–D10, is strongly inhibited by D_2. With higher D_2 pressures, the surface coverage of D on the Pt will be higher and fewer empty sites will be available. The inhibition of the rollover by D_2 therefore implies that an extra (empty) adsorption site is required for the rollover mechanism.

In summary, a positive first order in CP and a negative order of -0.85 in D_2 were found. The selectivities were independent of the CP partial pressure, and a kinetic model with corresponding reaction rate was developed. Increasing D_2 pressures lead to an enhanced rotation of the π-η^2 intermediate, which is in agreement with the proposed rotation mechanism (Fig. 6). In addition, a decreased rollover selectivity is observed, which implies that the rollover mechanism via the di-σ-η^1 intermediate requires an empty adsorption site.

4.2. Effect of temperature

The Arrhenius plot shown in Fig. 5A represents a rate-determining step during the H/D exchange with an apparent activation energy of $E_{app} = 55$ kJ/mol. According to the mechanism proposed above, the selectivity is determined in the subsequent mechanisms following the adsorption.

As shown in Fig. 5B, the effect of increasing the temperature on the selectivity is a decrease for D1 and D2 accompanied by an increase for D6–D10. The relative amounts of

Table 3
The effect of temperature on the exchange selectivity. Where the data given are based upon the Monte Carlo model (only the two extreme temperatures are given, the other temperatures are shown in Fig. 5B)

T (°C)	Selectivity (%) towards intermediate[a]						
	σ-η^1	di-σ-η^2	π-η^2				
	(D1)	(D2)	(D2)	(D3)	(D4)	(D5)	di-σ-η^1 (> D6)
66	22.6	3.3	4.8	8.0	9.1	33.1	19.1
81	16.2	1.9	4.3	7.3	8.4	33.2	28.8

[a] For a description of the intermediates: see Fig. 1.

D3–D5 are unaffected. This is similar to what is observed in the literature [32,39].

The large number of rotations (∼18 for the D5 product, Table 1) and the observation that the selectivity towards D3–D5 is unaffected by temperature indicate that the rotation mechanism is virtually nonactivated.

The selectivity for the rollover, leading to D6–D10, increases from 19.1% at 66 °C to 28.8% at 81 °C (see Table 3 and Fig. 5B). This increase shows that the rollover mechanism is an activated mechanism. As explained earlier, it is the π-η^2 intermediate (Fig. 1C) that rolls over via the di-σ-η^1 intermediate, and the activity is given by formula (6). Since this activity is as high as $28.8/81.2 = 35\%$, the activity for rollover is no longer differential. This can be corrected by assuming that 35% of the rolled-over molecules rollover again and then the activity is approximately (35% from 35%) $+ 35\% = 47\%$. By constructing an Arrhenius plot of this corrected fraction as a function of temperature the activation energy for rollover can be estimated (Fig. 9). The apparent activation energy for rollover was estimated at 24 kJ/mol.

4.3. Implications for the H/D exchange experiments

In the older literature, the selectivities as measured were used to describe the experiments. It has been shown that this is not adequate. If one wants to investigate the relative contributions of the four competing exchange mechanisms to the selectivity, it is essential to carefully investigate the observed selectivity. For example, when a molecule containing 5 D atoms is observed, in reality it has undergone as much as

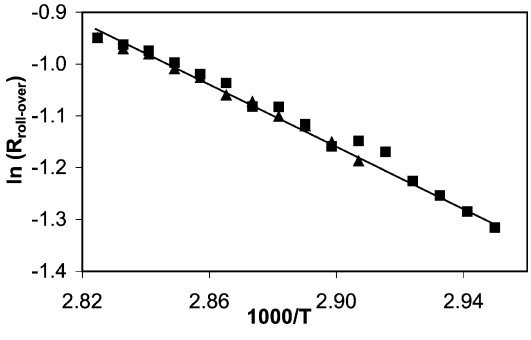

Fig. 9. Arrhenius plot of the influence of temperature on the selectivity toward rollover.

∼20 exchange steps, 15 of which are D/D exchanges. The developed Monte Carlo model is essential to calculate this true number of exchange steps based upon the observed selectivity. Each exchange step is associated with a rotation of the π-η^2 intermediate to an adjacent C–C bond in CP. This rotation mechanism cannot proceed via an interconversion of the σ-η^1 intermediate (Fig. 1A) on the one hand and di-σ-η^2 (Fig. 1B) and π-η^2 (Fig. 1C) intermediates on the other hand. Instead, the rotation mechanism is hardly activated and proceeds via an allylic-like mechanism (Fig. 6). Also, two different exchange mechanisms proceeding via the di-σ-η^2 (Fig. 1B) and π-η^2 (Fig. 1C) intermediates result in the D2 product. The relative contributions can only be calculated with this Monte Carlo model. This Monte Carlo model is also essential in determining the true rollover activity.

5. Conclusions

The H/D exchange of CP leads to a product distribution with maxima for the D1, D5, and D10 products. The observed exchange patterns can be simulated by a newly developed Monte Carlo-based model. At least four different mechanisms lead to the observed product distributions. The Monte Carlo model reveals that the real number for exchange steps cannot be directly extracted from the measured exchange pattern. For example, the D5 product indicates that five exchange steps have occurred. In reality, however, the number of exchange steps can be as high as 15–20. The mechanism leading to the D5 product is proposed to proceed via a rotation mechanism involving a allylic mechanism and a π-η^2 intermediate. Careful considerations regarding the observed selectivity inevitably lead to the conclusion that D2 is produced via two different intermediates, whose relative contributions are given by the Monte Carlo model. In addition, it is concluded that the rollover leading to the D6–D10 products can only occur when the CP first is adsorbed as the π-η^2 intermediate, followed by a rollover via the di-σ-η^1 intermediate. Again the Monte Carlo model is essential to obtain the true activity for this rollover. In addition to an understanding of origins of the selectivity, a kinetic model describing the activity and orders in reactants was also developed. The exchange pattern, or selectivity, is determined in a series of reactions occurring *after* the rate-determining step.

Appendix A

The reactions considered are:

$$C_5H_{10}(g) + {}^* \xleftrightarrow{K_1} C_5H_{10}({}^*), \quad \text{(I)}$$

$$D_2(g) + 2{}^* \xleftrightarrow{K_2} 2D({}^*), \quad \text{(II)}$$

$$C_5H_{10}({}^*) + {}^* \xrightarrow{k_{+3}} C_5H_9({}^*) + H({}^*), \quad \text{(IIIA)}$$

$$C_5H_nD_{9-n}({}^*) + D({}^*) \xrightarrow{k_{-3}} C_5H_nD_{10-n}({}^*), \quad \text{(IIIB)}$$

with *, an empty adsorption site, and D$(^*)$, an adsorbed atom of deuterium (D_2). Since H_2 and D_2 are chemically similar, H$(^*)$ = D$(^*)$ and $C_5H_nD_{9-n}(^*) = C_5H_9(^*)$, and thus k_{+3} and k_{-3} are equal in a steady state. Between reactions (IIIA) and (IIIB), the cyclopentane can exchange a lot of D atoms.

The accompanying reaction rates are

$$R_1 = r_{+1} - r_{-1} = k_{+1} P_{CP} \theta_* - k_{-1} \theta_{C_5H_{10}} \quad (A.1)$$

$$R_2 = r_{+2} - r_{-2} = k_{+2} P_{D_2} \theta_*^2 - k_{-2} \theta_D^2 \quad (A.2)$$

$$R_3 = r_{+3} - r_{-3} = k_{+3} \theta_{C_5H_{10}} \theta_* - k_{-3} \theta_{C_5H_9} \theta_H \quad (A.3)$$

with θ_x, the fractional coverage of species X; k the reaction constants with the equilibrium constant $K_n = k_{+n}/k_{-n}$.

Since H_2 and D_2 are chemically similar, H$(^*)$ = D$(^*)$. Substituted into R_3, this gives

$$R_3 = r_{+3} - r_{-3} = k_{+3} \theta_{C_5H_{10}} \theta_* - k_{-3} \theta_{C_5H_9} \theta_D. \quad (A.4)$$

Furthermore, the total coverage is 1:

$$1 = \theta_* + \theta_{C_5H_{10}} + \theta_{C_5H_9} + \theta_D. \quad (A.5)$$

Since all measurements are performed in steady state, the coverages are constant in time:

$$\frac{d\theta_{C_5H_9}}{dt} = 0 = k_{+3} \theta_{C_5H_{10}} \theta_* - k_{-3} \theta_{C_5H_9} \theta_D,$$
$$\rightarrow \theta_{C_5H_9} = \frac{k_{+3} \theta_{C_5H_{10}} \theta_*}{k_{-3} \theta_D} = \frac{K_3 \theta_{C_5H_{10}} \theta_*}{\theta_D}, \quad (A.6)$$

$$\frac{d\theta_{C_5H_{10}}}{dt} = 0 = k_{+1} P_{CP} \theta_* - k_{-1} \theta_{C_5H_{10}} - k_{+3} \theta_{C_5H_{10}} \theta_* + k_{-3} \theta_{C_5H_9} \theta_D, \quad (A.7)$$

$$\frac{d\theta_D}{dt} = 0 = k_{+2} P_{D_2} \theta_*^2 - k_{-2} \theta_D^2 + k_{+3} \theta_* \theta_{C_5H_{10}} - k_{-3} \theta_{C_5H_9} \theta_D. \quad (A.8)$$

Substitution of (A.6) into (A.7) leads to

$$\theta_{C_5H_{10}} = K_1 P_{CP} \theta_*; \quad (A.9)$$

substitution of (A.7) and (A.9) into (A.8) leads to

$$\theta_D = \theta_* * \sqrt{K_2 P_{D_2}}; \quad (A.10)$$

and substitution of (A.6), (A.9), and (A.10) into (A.5) gives

$$\theta_* = \frac{1}{1 + K_1 P_{CP} + \frac{K_1 K_3 P_{CP}}{\sqrt{K_2 P_{D_2}}} + \sqrt{K_2 P_{D_2}}}. \quad (A.11)$$

Since all cyclopentane which dissociates on the surface is detected as a D1–D10 product, the reaction rate is given by r_{+3} or r_{-3}

$$R = r_{-3} = k_{-3} \theta_{C_5H_9} \theta_D = k_{-3} \frac{K_3 \theta_{C_5H_{10}} \theta_*}{\theta_D} \theta_D$$
$$= k_{-3} K_1 K_3 P_{CP} \theta_*^2$$
$$= \cdots = \frac{k_{-3} K_1 K_3 P_{CP}}{\left(1 + K_1 P_{CP} + \frac{K_1 K_3 P_{CP}}{\sqrt{K_2 P_{D_2}}} + \sqrt{K_2 P_{D_2}}\right)^2}. \quad (A.12)$$

Estimation of reaction constants:

1. Reaction (I) is easy and fast, with $K_1 = k_{+1}/k_{-1} > 1$;
2. Reaction (II) is very fast, $K_2 \gg 1$;
3. Reaction (III) is the rate-determining step, thus $(k_{-3}, k_{+3}) \ll (k_{+1}, k_{-1}, k_{+2})$.

Thus, if $K_2 \gg K_1 K_3$, Eq. (A.12) can be simplified by ignoring several terms

$$R = \frac{k_{-3} K_1 K_3 P_{CP}}{\left(1 + K_1 P_{CP} + \frac{K_1 K_3 P_{CP}}{\sqrt{K_2 P_{D_2}}} + \sqrt{K_2 P_{D_2}}\right)^2} \approx \frac{k_{-3} K_1 K_3 P_{CP}}{K_2 P_{D_2}}.$$

References

[1] T.M. Tri, J. Massardier, P. Gallezot, B. Imelik, Stud. Surf. Sci. Catal. 11 (1982) 141.
[2] W.C. Neikam, M.A. Vannice, in: J.W. Mightower (Ed.), Proceedings of 5th International Congress on Catalysis, Palm Beach, 1972, Vol. 1, North-Holland, Amsterdam, 1973, p. 609.
[3] D. Poondi, M.A. Vannice, J. Catal. 161 (1996) 742.
[4] V.N. Romannikov, K.G. Ione, J. Catal. 66 (1980) 121.
[5] A. de Mallmann, D. Barthomeuf, J. Chim. Phys. 87 (1990) 535.
[6] R.A. Dalla Betta, M. Boudart, in: J.W. Mightower (Ed.), Proceedings of 5th International Congress on Catalysis, Palm Beach, 1972, North-Holland, Amsterdam, 1973, p. 1329.
[7] C. Besoukhanova, J. Guidot, D. Barthomeuf, J. Chem. Soc. Faraday Trans. I 77 (1981) 1595.
[8] A. de Mallmann, D. Barthomeuf, Stud. Surf. Sci. Catal. 46 (1989) 429.
[9] Z. Zhang, T.T. Wong, W.M.H. Sachtler, J. Catal. 128 (1991) 13.
[10] B.L. Mojet, J.T. Miller, D.E. Ramaker, D.C. Koningsberger, J. Catal. 186 (1999) 373.
[11] D.C. Koningsberger, J. de Graaf, B.L. Mojet, D.E. Ramaker, J.T. Miller, Appl. Catal. A Gen. 191 (2000) 205.
[12] D.E. Ramaker, J. de Graaf, J.A.R. Van Veen, D.C. Koningsberger, J. Catal. 203 (2001) 7.
[13] C. Hippe, R. Lamber, G. Schulz-Ekloff, U. Schubert, Catal. Lett. 43 (1997) 195.
[14] V.B. Kazansky, V.Yu. Borovkov, Stud. Surf. Sci. Catal. 92 (1995) 275.
[15] M.T.M. Koper, R.A. van Santen, S.A. Wasileski, M.J. Weaver, J. Chem. Phys. 113 (2000) 4392.
[16] A.Yu. Stakheev, E.S. Shapiro, N.I. Jaeger, G. Schulz-Ekloff, Catal. Lett. 32 (1995) 147.
[17] M. Vaarkamp, B.L. Mojet, F.S. Modica, J.T. Miller, D.C. Koningsberger, J. Phys. Chem. 99 (1995) 16067.
[18] J. de Graaf, Thesis, Utrecht University, Ridderkerk, 2001.
[19] G.C. Bond, M.A. Keane, H. Kral, J.A. Lercher, Catal. Rev. Sci. Eng. 42 (2000) 323.
[20] K. Foger, J.R. Anderson, J. Catal. 54 (1978) 318.
[21] Z. Karpinski, S.N. Gandhi, W.M.H. Sachtler, J. Catal. 141 (1993) 337.
[22] R. Burch, Z. Paál, Appl. Catal. A Gen. 114 (1994) 9.
[23] R. Burch, Catal. Today 10 (1997) 233.
[24] M.J.P. Botman, K. de Vreugd, H.W. Zandbergen, R. de Block, V. Ponec, J. Catal. 116 (1989) 467.
[25] A. Khodakov, N. Barbouth, Y. Berthier, J. Oudar, P. Schulz, J. Chem. Soc. Faraday Trans. 91 (1995) 569.
[26] V. Eskinazi, R.L. Burwell, J. Catal. 79 (1983) 118.
[27] B.F. Hegarty, J.J. Rooney, J. Chem. Soc. Faraday Trans. I 85 (1989) 1861.

[28] T. Baird, E.J. Kelly, W.R. Patterson, J.J. Rooney, J. Chem. Soc. Chem. Commun. (1992) 1431.
[29] A. da Costa Faro Jr., C. Kemball, J. Chem. Soc. Faraday Trans. 91 (1995) 741.
[30] J.K.A. Clarke, B.F. Hegarty, J.J. Rooney, J. Mol. Catal. 62 (1990) L39–L43.
[31] Y. Inoue, J.M. Hermann, H. Schmidt, R.L. Burwell, J.B. Butt, J.B. Cohen, J. Catal. 53 (1978) 401.
[32] R. Pitchai, S.S. Wong, N. Takahashi, J.B. Butt, R.L. Burwell, J.B. Cohen, J. Catal. 94 (1985) 478.
[33] E.J. Kelly, W.R. Patterson, J.J. Rooney, J. Mol. Catal. 89 (1994) 19.
[34] C. Kemball, Adv. Catal. 11 (1959) 223.
[35] V. Ponec, G.C. Bond, Catalysis by Metals and Alloys, in: Studies in Surface Science and Catalysis, Vol. 95, Elsevier, Amsterdam, 1995.
[36] M.K. Oudenhuijzen, J.H. Bitter, D.C. Koningsberger, J. Phys. Chem. B 105 (2001) 4616.
[37] M.K. Oudenhuijzen, P.J. Kooyman, B. Tappel, J.A. van Bokhoven, D.C. Koningsberger, J. Catal. 205 (2002) 135.
[38] R.A. van Santen, P.W.N.M. van Leeuwen, J.A. Moulijn, B.A. Averill, Catalysis: An Integrated Approach, 2nd ed., in: Studies in Surface Science and Catalysis, Vol. 123, Elsevier Science, Amsterdam, 1999.
[39] V. Ponec, W.M.H. Sachtler, J. Catal. 24 (1972) 250.
[40] R.L. Burwell, Acc. Chem. Res. 2 (1969) 289.
[41] E. Poulain, V. Bertin, S. Castillo, A. Cruz, J. Mol. Catal. A 116 (1997) 385.
[42] B. Hammer, J.K. Nørskov, Surf. Sci. 343 (1995) 211.
[43] B. Hammer, J.K. Nørskov, Nature 376 (1995) 238.
[44] J. Barbier, E. Lamy-Pitara, P. Marecot, Bull. Soc. Chim. Belg. 105 (1996) 99.
[45] K. Schrage, R.L. Burwell, J. Am. Chem. Soc. 88 (1966) 4549.
[46] J.T. Campbell, C.T. Campbell, Surf. Sci. 210 (1989) 46.